

A Dual Quadrupole Trap for Molecular Spin-Flip Loss

David Reens, Hao Wu, Tim Langen, and Jun Ye
Physics Department, University of Colorado at Boulder

(Dated: March 6, 2017)

A new electromagnetic trap geometry allows full tuning of complex molecular spin-dynamics in crossed electric and magnetic fields. If not tuned properly, these dynamics lead to spin-flip loss that afflicts a wide set of candidate molecules. The spin-flip loss can be significant even above 100 mK and increases with $1/T$, so its removal represents a critical step toward ultracold molecules. The trapping geometry features a 0.5 K trap depth and 5 T/cm trap strength, and allows spin-dynamics to be tuned with only an external bias coil. Spin-flip loss is tuned in a 170 mK sample of OH molecules from over 200 s $^{-1}$ to below the vacuum limited lifetime of 2 s $^{-1}$.

The ultracold regime extends toward molecules on many fronts [1]. Several bialkali molecules are available [2–4] and others are under development. Creative and carefully engineered laser cooling strategies are tackling certain nearly vibrationally diagonal molecules [5–9]. A plethora of non-optical cooling strategies have succeeded to greater or lesser extents on other molecules [10–14]. All of these molecules will require secondary strategies like evaporation or sympathetic cooling to make further gains in phase space density. They also may face a familiar challenge: spin flip loss near the zero of a magnetic trap, but dramatically enhanced for many doubly dipolar molecules due to their internal spin dynamics in mixed electric and magnetic fields.

The knowledge of spin flips or Majorana hops as an eventual trap lifetime limit predates the very first magnetic trapping of neutrals [15]. Spin flips were directly observed near 10 μ K and overcome in the TOP trap [16], and soon later with a plugged dipole trap [17], famously enabling the first Bose-Einstein condensates. We first observed spin-flips in a 45 mK OH sample, three orders of magnitude higher in temperature compared with the atomic case. The observation was discussed briefly in the appendix of [18], and a representative data trace is shown in fig. 1, panel (f). We will begin with an explanation of the internal spin-dynamics that lead to this behavior in the specific geometry of a 3D quadrupole magnetic trap with superposed homogeneous electric field. Our fully general results will then be applied to explain our new trapping geometry and how it achieves tunable removal of spin-flip loss. We note that mixed fields are an inevitable component of any experiment which seeks to take advantage of the doubly dipolar nature of molecules.

The internal spin-dynamics that lead to this enhanced spin-flip loss are subtle. So much so that they have eluded two previous investigations of note. In [21] the analogues of atomic spin-flip loss for molecules in mixed fields were investigated, and the case of a magnetic quadrupole trap for OH molecules with superposed electric field was specifically addressed. It was concluded that no significant loss enhancement relative to the atomic case should be evident. While this is true for the approximate $^2\Pi_{1/2}$

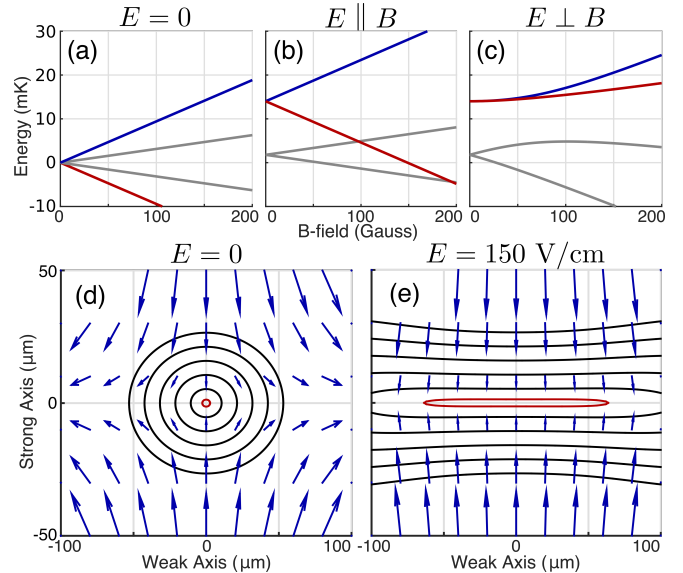


FIG. 1. The blocking effect. (a), four Zeeman split lines in the ground state of OH. A nearly identical set of four states of opposite parity lie 100 mK below. The trapped state and its spin flip partner are in blue and red. (b) Zeeman splitting with the addition of an electric field of 150 V/cm parallel to the magnetic field. (c) Again but with the fields orthogonal. The red state, untrapped in parallel fields, here draws very close to the trapped state in blue. A surface showing the behavior at all angles can be found in [18]. (d) Contours of energy separation every 2 mK between the trapped and spin-flipped state near the zero of a 2 T/cm magnetic quadrupole trap without electric field. Magnetic field arrows in blue. (e) Again with 150 V/cm. Note the drastic widening of the lowest contour, in red. Here the vectors point along the direction of the local Hund's Case X quantization axis [19] and their magnitude gives the local potential energy of the trapped state relative to the trap center.

Hamiltonian used in that study, it is not true for the actual $^2\Pi_{3/2}$ ground state of OH. In [19], it was correctly noted that Hund's case (a) molecules maintain a quantization axis in mixed fields. In fact the various ground states of the molecule align with a quantization axis that is either the vector sum or the vector difference of the

dipole moment weighted electric and magnetic fields. It was asserted that this would maintain quantization near the zero of a quadrupole trap and avoid spin-flip loss. Although quantization is indeed maintained, this actually furthers the spin-flip loss instead of hindering it.

This is in fact the crux of the internal spin-dynamics that can lead to loss. With only magnetic field, an atom or molecule remains trapped only insofar as it can adiabatically follow the direction of the field. Near the center of a quadrupole trap, the direction changes the most rapidly, and loss can occur. When homogeneous electric field is added, it dominates in the trap center where the magnetic field is weakest. Quantization is maintained but the quantization axis does not rotate with the magnetic field as it needs to. Further away from the trap center the molecule is then strong field seeking with respect to the magnetic field and is lost. The reason that quantization can be maintained without remaining in the trapped substate is that the molecules actually need to switch from the vector sum quantization axis to the vector difference quantization axis, so as to always be doubly weak field seeking regardless of whether the fields point towards or away from one another. [20]

In terms of eigenstate energies, this manifests as a very narrow splitting between the magnetically weak and strong field seeking substates in the region where the magnetic field's projection on the electric changes sign, i.e. where they are orthogonal. In a perfect quadrupole with superposed homogeneous electric field, this region is a perfect plane, but even in a more general geometry, it is necessarily a two dimensional region since it is a level set of the scalar $\phi = E \cdot B$ defined on the entire volume of interest. In the subset of this plane where $\mu_B B < d_E E$, the Zeeman effect is not linear but is instead reduced in efficacy to cubic order. We call this effect "blocking", see fig. 1, and we say that the electric field blocks the Zeeman effect from linear to cubic in the orthogonal plane.

Based on this observation, we numerically evaluate the loss rates and enhancements for a thermal molecule distribution by performing an integral of the flux through the loss plane weighted by the Landau-Zener hopping probability. This is described more fully in the appendix, and is a significant improvement over previous attempts to evaluate this loss. The results are tabulated as follows:

TABLE I. Enhancements and loss rates for OH

E field	45 mK		5 mK		Purpose
	ν	$\Gamma(s^{-1})$	ν	$\Gamma(s^{-1})$	
0 V/cm	1	0.02	1	1.3	No Field
10 V/cm	1	0.02	2	2.5	Stray Field
300 V/cm	5	0.1	9	11	Evaporation
550 V/cm	17	0.3	40	50	Spectroscopy
3 kV/cm	1000	19	1600	2000	Polarizing

These electric field magnitudes correspond to those used in our experiment as a spectroscopic tool as described in [22] and as an evaporative knife in [23]. Given our typical experiment length of 100 ms, the spin-dynamical effect associated with these field magnitudes is negligible at initial temperatures, but relevant at the final ensemble temperatures targeted during evaporation. For this and other reasons, it is evident that 5 mK temperatures were not attained, although it does seem that some phase space compression was achieved for 20 mK evaporation sequences.

One obvious way to avoid the loss enhancement is to simply never use electric field in a magnetic trap. This prevents loss from being enhanced compared with atoms, but doesn't remove it entirely. Another possibility is to trap with electric fields, where no spin-flip loss is possible thanks to the $\Delta = h \cdot 1.67$ GHz splitting between the weak and strong field seeking states. However this splitting also results in a significant reduction in trap gradient close to the center, very undesirable for further cooling by evaporation. Moreover, there are reductions in inelastic to benefit from in magnetic fields. [23]

Seeking to remove the loss entirely but without trap gradient sacrifice, we switch from a 3D to a 2D magnetic trap, and use an intersecting electric 2D quadrupole to plug the remaining direction (and incidentally add strength to one of the already trapped directions). This does not prevent $E \perp B$, but it allows us to tune the minimum B field with an external bias coil oriented along the axis of the 2D quadrupole trap. This is similar to the Ioffe-Pritchard strategy [24], where a 2D quadrupole is combined with an axial dipole trap. Typically, the axial and radial trapping interfere somewhat, resulting in significantly lower trap depths compared to the 3D quadrupole. We thwart this interference by the use of different fields for the axial and radial directions, which can "block" one another as discussed earlier but never result in an absolute decrease in potential energy of the doubly weak field seeking substate.

Serendipitously, we are able to achieve these fields with a geometry that exactly matches that of our Stark decelerator [13], as shown in fig. 2. OH molecules are created using a supersonic expansion source and decelerated from an initial velocity of 460m/s to a final velocity of 40ms/s using a Stark decelerator. The decelerator contains 142 electrode pairs. By magnetizing a pair of such pins in a dual domain manner, a 2D quadrupole is formed. The electric trapping in the third direction as achieved by charging the pin pair previous and following the magnetic pins to the same voltage, requiring only that high voltage switches be cascaded since normally pin pairs are oppositely charged. By intuition and by our phase space coupling simulations, this represents a near best-case scenario for coupling between a pulsed decelerator and a trap, although in practice we do not realize any significant molecule number increase relative

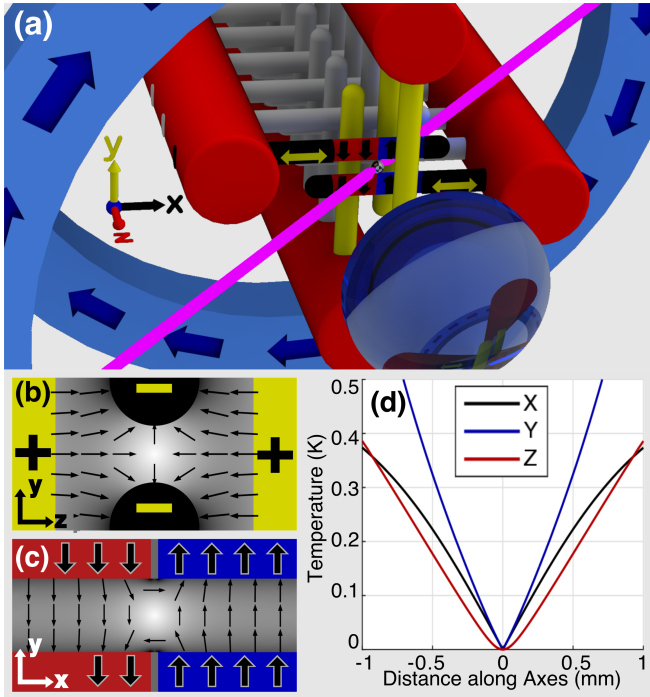


FIG. 2. Trapping is achieved by combining a radial magnetic quadrupole field, created by the magnetized second to last electrode pair of the decelerator, with a longitudinal electric quadrupole field created by the third to last and last electrode pairs, respectively (yellow, one electrode is omitted for clarity). The magnetized electrodes can be translated *in situ* along the x-axis to align their domains and optimize the quadrupole. As there is no trapping magnetic field in the z-direction in this configuration, macroscopic external bias coils can be used to lift the gap between the top two states of the OH ground-state manifold and thus tune the molecular loss. Detection is realized using laser induced fluorescence along the x+y+z direction (blue), which is collected using a lens system and PMT in the z-direction.

to our previous geometries. This could be related to the difficulty of conditioning the magnet surfaces. For N38 magnets chosen so as to maintain magnetization during violent conditioning procedures, $B' = 5 \text{ T/cm}$ and $E' = 100 \text{ kV/cm}^2$. These correspond to trap frequencies $\nu_x = 3 \text{ kHz}$, $\nu_y = 5 \text{ kHz}$, and $\nu_z = 4 \text{ kHz}$ for molecules traveling on the axes.

Now regarding the molecule enhanced spin-flip loss, $E \perp B$ on a hyperbolic sheet which deviates more significantly from the z axis with increasing B_{coil} , and reduces to the pair of planes $x = 0$ and $y = 0$ in the limit that $B_{\text{coil}} = 0$. On this hyperbolic sheet, B must be larger than the threshold set by Eq. ?? to overcome blocking. Fortunately, B_{coil} does not have to overcome the blocking limit, it only needs to push the $B \perp E$ surface slightly off the z-axis for the strong quadrupole fields to overcome the blocking. In fig. 3, the surfaces where $B \perp E$ are colored wherever the splitting there is below the threshold κ . Note how B_{coil} tunes the proximity of the loss regions

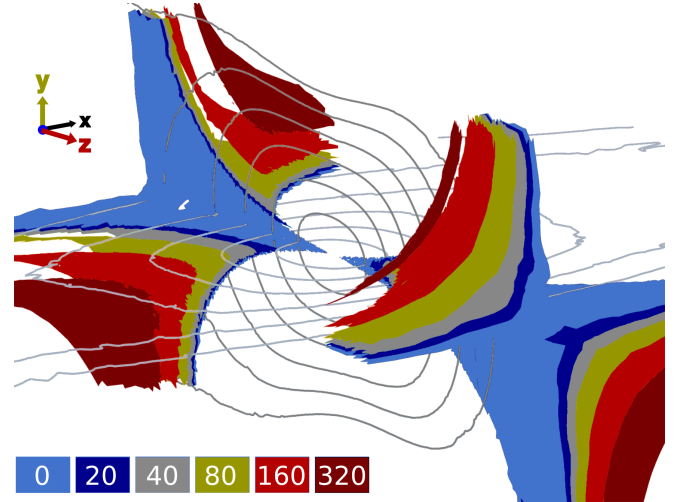


FIG. 3. Each color shows the surfaces where spin-flip can occur for the particular value of B_{coil} given by the legend in units of Gauss. Trap energy contours are shown in gray. Larger B_{coil} pushes the loss regions away from the trap center.

to zero. The loss regions are never fully removed, but they can be tuned high enough that molecules accessing them could already escape the trap mechanically.

Unfortunately, the preceding picture only applies for well-aligned magnetic pins. Translations of our magnetic pins in their mounts lead to important modifications to the axial behavior of the magnetic trap that influence the tunability of the loss. Essentially, when the pairs of magnetic domains of the two pins are out of mutual alignment by a distance d , a small trapping field $\vec{B} \propto B' z \hat{z}$ is introduced along the otherwise magnetic-field-free z-axis. This means that B_{coil} no longer directly tunes the minimum magnetic field in the trap. Instead, B_{coil} must first overcome the slight trapping field along the z-axis, translating a point of zero field along the z axis and eventually out of the trap. In order to really disentangle this effect from our results, we installed an *in-situ* pin translation stage and obtained the family of curves shown in fig. 4. With the pins tuned into alignment, B_{coil} of either sign suppresses the loss in agreement with fig. 3. Otherwise, B_{coil} first increases the loss by moving the magnetic zero into regions of large electric field, but eventually overwhelms it, producing a characteristic double-well shape.

As a quantitative companion to this intuition for the double-well structure, we fit the family of curves shown in fig. 4 by performing a detailed numerical integration of spin-flip loss flux over all hyperbolic planes where loss can occur, weighted by the expected Maxwell-Boltzmann distribution of molecules in the trap. The computation is performed in COMSOL Multiphysics, with cloud temperature as the only free parameter. Source-code for the model is available.[?]. The fit temperature is approximately $100 \pm 10 \text{ mK}$. This temperature is twice that of

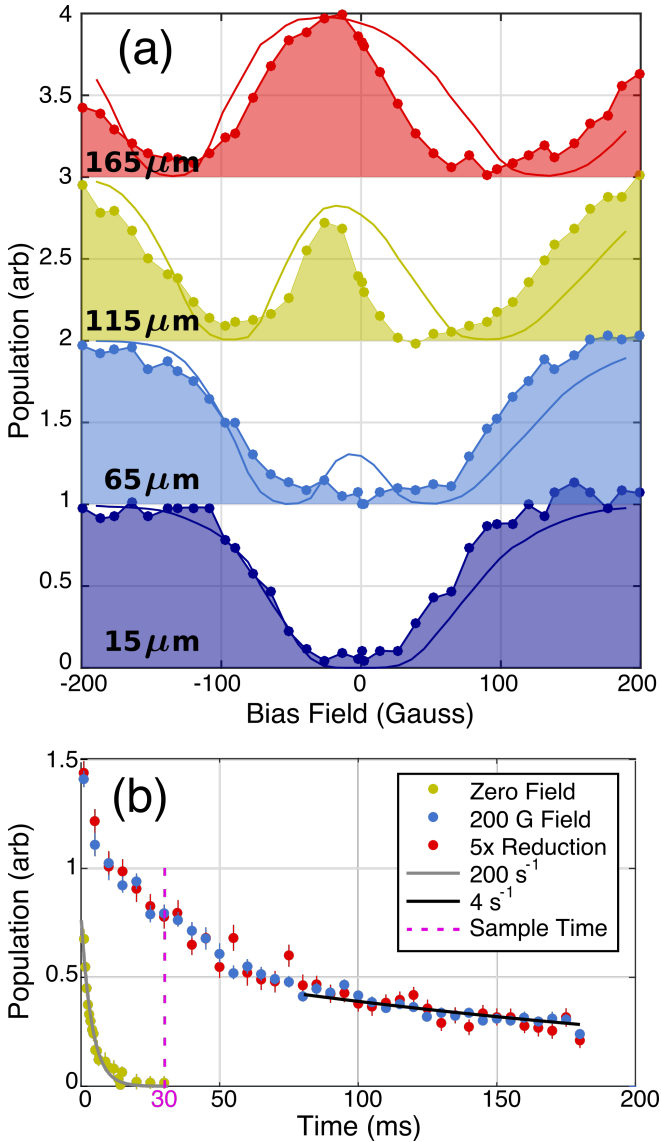


FIG. 4. Family of curves showing the remaining population after 30ms as a function of pin offset and magnetic bias field.

our previous traps, most likely due to the increased trap depth but potentially related to conditioning challenges for the magnetic pins.

To further validate the claim that B_{coil} tunes loss away from the trap center, we perform a Zeeman microwave spectroscopy along the $|f, 3/2\rangle$ to $|e, 3/2\rangle$ line as in our previous work [23]. Rather than using a bias tee setup, a dangerous prospect with our trap deeply integrated in the high voltage decelerator, we use a home-made microwave probe to directly excite free space cavity modes of our vacuum chamber. The results are shown in fig. 5. With the magnetic pins aligned, it is seen that higher values of B_{coil} indeed increases the population of molecules able to survive at higher fields. In order to perform this spectroscopy, the trapping electric fields are switched off im-

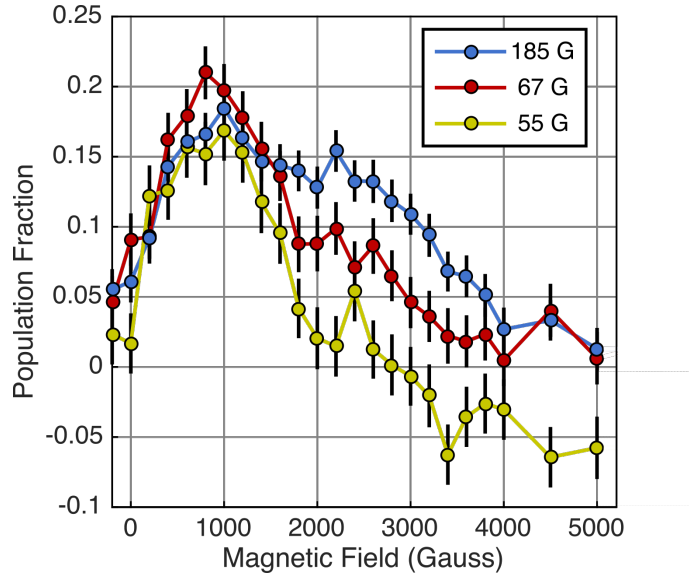


FIG. 5. Microwave Thermometry in the trap.

mediately prior to the application of a microwave transfer pulse tuned to a particular magnetic field strength. Thus the results reflect the Zeeman potential energy only. Roughly speaking, the average field of 2 kG corresponds to 200 mK for OH. Since this is approximately half the potential energy, we have $U \approx 400$ mK. From the virial theorem for a linear trap, $U = 4.5k_B T$, so we can say the spectrum is consistent with $T \approx 90$ mK and consistent with our fitting in fig. 4.

In the case of lowest applied magnetic field in fig. 5, i.e. deepest cutting of the loss region toward the trap center, a negative going signal is observed. This indicates a build-up in the opposite parity $|e, 3/2\rangle$ state. Although the spin-flips we have discussed connect $|f, \pm 3/2\rangle$, the $|f, -3/2\rangle$ state actually remains trapped thanks to adiabatic transitions to $|f, 1/2\rangle$ and later $e, 3/2\rangle$ facilitated by the large E fields present in the trap. This secondary state is much more weakly trapped and exhibits molecule enhanced spin-flip loss to other lower states, although the enhancement is related to a quadratic blocking of the zeeman splitting near the intersection of $|f, -3/2\rangle$ and $|f, 1/2\rangle$, and is thus not as dominating as the loss in the primary state due to cubic blocking.

Once the loss is fully removed, we observe the trend shown in fig. ???. The decay rate decreases with population over a timescale that is long compared with trap frequency and is thus suggestive of a collisional process. However, we implement a completely phase-space blind density reduction technique to significantly reduce our molecule number and observe little change in the shape of the trend, indicating that primarily single-particle physics is responsible. We suspect that the trend is related to the persistence of high energy chaotic orbits which can possess long escape times, as seen in other ex-

otically shaped trapping potentials [25]. We hope in the near future to implement an increase in molecule number rather than a decrease, by means of a suite of density enhancing experimental improvements slated to come online.

We have conclusively demonstrated the existence of molecule enhanced spin-flip loss by tuning it from an overwhelming rate to complete removal. Our explanation of the loss provides detailed predictions of how its position and magnitude ought to scale with bias field and trap alignment, which we have experimentally verified. Our results contradict existing predictions about molecule enhanced spin-flip loss and we provide a consistent framework that explains this. Beyond merely demonstrating the loss, we have devised a viable trapping geometry in which it is fully mitigated without trap-depth sacrifice, paving the way toward further improvements in molecule trapping and cooling.

$$\vec{B} = B'y\hat{x} + B'x\hat{y} + B_{coil}\hat{z} \quad (1)$$

$$\vec{E} = E'y\hat{y} - E'z\hat{z} \quad (2)$$

$$\vec{B} \cdot \vec{E} = 0 \quad (3)$$

$$B'x E'y - B_{coil} E'z = 0 \quad (4)$$

$$B_{coil} z = xy B' \quad (5)$$

$$\gamma_{\text{flip}} = \frac{\int_0^{\infty} 2\pi r e^{-r/r_0} \int_{-\infty}^{\infty} e^{-mv_z^2/kT} |v_z| e^{-2\pi\Gamma(r,v_z)} dv_z dr}{\int_0^{\infty} 2\pi r e^{-r/r_0} \int_{-\infty}^{\infty} e^{-mv_z^2/kT} dv_z dr} \quad (6)$$

-
- [1] L. D. Carr, D. DeMille, R. V. Krems, and J. Ye, *New Journal of Physics* **11**, 055049 (2009).
 - [2] K.-K. Ni, S. Ospelkaus, M. H. G. de Miranda, A. Pe'er, B. Neyenhuis, J. J. Zirbel, S. Kotchigova, P. S. Julienne, D. S. Jin, and J. Ye, *Science* **322**, 231 (2008).
 - [3] T. Takekoshi, L. Reichsöllner, A. Schindewolf, J. M. Hutson, C. R. Le Sueur, O. Dulieu, F. Ferlaino, R. Grimm, and H.-C. Nägerl, *Physical Review Letters* **113**, 205301 (2014).
 - [4] J. W. Park, S. A. Will, and M. W. Zwierlein, *Physical Review Letters* **114**, 205302 (2015).
 - [5] M. H. Steinecker, D. J. McCarron, Y. Zhu, and D. DeMille, *ChemPhysChem* **17**, 3664 (2016).
 - [6] J. F. Barry, D. J. McCarron, E. B. Norrgard, M. H. Steinecker, and D. DeMille, *Nature* **512**, 286 (2014).

- [7] B. Hemmerling, E. Chae, A. Ravi, L. Anderegg, G. K. Drayna, N. R. Hutzler, A. L. Collopy, J. Ye, W. Ketterle, and J. M. Doyle, *Journal of Physics B: Atomic, Molecular and Optical Physics* **49**, 174001 (2016).
- [8] M. T. Hummon, M. Yeo, B. K. Stuhl, A. L. Collopy, Y. Xia, and J. Ye, *Physical Review Letters* **110**, 143001 (2013).
- [9] V. Zhelyazkova, A. Cournol, T. E. Wall, A. Matsushima, J. J. Hudson, E. A. Hinds, M. R. Tarbutt, and B. E. Sauer, *Physical Review A* **89**, 053416 (2014).
- [10] J. M. Doyle, J. D. Weinstein, R. DeCarvalho, T. Guillet, and B. Friedrich, *Nature* **395**, 148 (1998).
- [11] A. Prehn, M. Ibrügger, R. Glöckner, G. Rempe, and M. Zeppenfeld, *Physical Review Letters* **116**, 063005 (2016).
- [12] H. L. Bethlem, G. Berden, and G. Meijer, *Physical Review Letters* **83**, 1558 (1999).
- [13] J. R. Bochinski, E. R. Hudson, H. J. Lewandowski, G. Meijer, and J. Ye, *Physical Review Letters* **91**, 243001 (2003).
- [14] N. Akerman, M. Karpov, L. David, E. Lavert-Ofir, J. Narevicius, and E. Narevicius, *New Journal of Physics* **17**, 065015 (2015).
- [15] A. L. Migdall, J. V. Prodan, W. D. Phillips, T. H. Bergeman, and H. J. Metcalf, *Physical Review Letters* **54**, 2596 (1985).
- [16] W. Petrich, M. H. Anderson, J. R. Ensher, and E. A. Cornell, *Physical Review Letters* **74**, 3352 (1995).
- [17] K. B. Davis, M. O. Mewes, M. R. Andrews, N. J. van Druten, D. S. Durfee, D. M. Kurn, and W. Ketterle, *Physical Review Letters* **75**, 3969 (1995).
- [18] B. K. Stuhl, M. Yeo, M. T. Hummon, and J. Ye, *Molecular Physics* **111**, 1798 (2013).
- [19] J. L. Bohn and G. Quéméner, *Molecular Physics* **111**, 1931 (2013).
- [20] The existence of the internal spin-dynamical effect was known and described in the appendix of [18], but more thorough recent investigations have demonstrated it to be of larger magnitude.
- [21] M. Lara, B. L. Lev, and J. L. Bohn, *Physical Review A* **78**, 033433 (2008).
- [22] B. K. Stuhl, M. Yeo, B. C. Sawyer, M. T. Hummon, and J. Ye, *Physical Review A* **85**, 033427 (2012).
- [23] B. K. Stuhl, M. T. Hummon, M. Yeo, G. Quéméner, J. L. Bohn, and J. Ye, *Nature* **492**, 396 (2012).
- [24] D. E. Pritchard, *Physical Review Letters* **51**, 1336 (1983).
- [25] R. González-Férez, M. Iñarrea, J. P. Salas, and P. Schmelcher, *Physical Review E* **90**, 062919 (2014).
- [26] T. H. Bergeman, P. McNicholl, J. Kycia, H. Metcalf, and N. L. Balazs, *Journal of the Optical Society of America B* **6**, 2249 (1989).
- [27] R. Golub and J. M. Pendleton, *Reports on Progress in Physics* **42**, 439 (1979).
- [28] D. E. Pritchard, *Physical Review Letters* **51**, 1336 (1983).
- [29] I. I. Rabi, *Physical Review* **49**, 324 (1936).
- [30] B. C. Sawyer, B. K. Stuhl, D. Wang, M. Yeo, and J. Ye, *Physical Review Letters* **101**, 203203 (2008).
- [31] M. Zeppenfeld, B. G. U. Englert, R. Glöckner, A. Prehn, M. Mielenz, C. Sommer, L. D. van Buuren, M. Motsch, and G. Rempe, *Nature* **491**, 570 (2012).